Transport of Swelling Penetrants in Glassy Polymers: Influence of Convection

G. C. SARTI, C. GOSTOLI, and G. RICCIOLI, *Istituto di Impianti Chimici, Facolta di Ingegneria, Universitá di Bologna, Italy,* and R. G. CARBONELL, *Department of Chemical Engineering, North Carolina State University, Raleigh, North Carolina 27695*

Synopsis

The transport of a solute by diffusion into a glassy polymer can lead to swelling of the material. For certain types of polymers, a sharp interface is formed between the swollen region and the glassy core. When the density of the swollen material is much smaller than the density of the glass, a significant convective mass-average velocity is generated within the sample. Previous models have neglected the role this convection plays in solute transport and in the proper calculation of the sample dimensions as a function of time. In this paper, we study the contribution of convective terms to the solute transport process, including the motion of the swollen polymer/solution interface. We also compute the eulerian strains that result from the calculated velocity fields and the stresses that would be generated if a linear viscoelastic model is used as a constitutive equation relating the stress to the strain. We show that serious errors can be generated in the calculations if convective terms are neglected. Furthermore, a comparison of the strains and stresses acting on the polymer with those acting on the mixture of solute and polymer shows that they can be significantly different. The stresses and strains acting on the polymer alone offer the most rational physical picture of the material deformation.

INTRODUCTION

When glassy polymers are exposed to both gaseous and liquid solutes, the resulting transport of solute into the matrix can lead to anomalous diffusion effects, so called because they differ from the expected behavior if the diffusion were purely fickian in nature. As the solute is absorbed into the polymer, swelling takes place, and depending on the mechanical and physical nature of the polymer-solute pair, a sharp front can be generated between the swollen and glassy regions.[1–4] The swelling and front formation result in curves of total mass of solute absorbed as a function of time, which deviate significantly from the expected square root of time behavior for fickian diffusion with a constant diffusivity. As the fronts meet, the rate of mass transport is often accelerated, and this is what distinguishes the super case II from the case II anomalous diffusion.

Even though the phenomenon is well documented, efforts to model the behavior of the diffusion and swelling process using physicochemical principles have led to various different approaches. For certain classes of polymers, it has been shown that the swollen polymer/glassy core front velocity can be related to the rate of crazing and its dependence on the stress acting at the interface.[5] The stress acting on the glassy polymer has been related to the osmotic pressure of the solute, and some effort has been made to

Journal of Applied Polymer Science, Vol. 32, 3627–3647 (1986)
 CCC 0021-8995/86/023627-21$04.00

include the effect of stresses normal to the diffusion direction by performing an overall force balance on the sample. In this type of model, the existence of a front is assumed a priori, and the remaining effort goes into generating a suitable constitutive equation for the front velocity and into calculating the diffusive flux in the swollen region. These moving front models[5–7] have been successful in explaining many of the observed phenomena, including super case II behavior.

Other researchers have attempted to develop models that would predict whether a front is formed.[8] In this approach, the tendency of the solute to swell the polymer is assumed to encounter a viscous resistance to the deformation. Depending on the magnitude of this resistance, the concentration profile in the solute can be either broad or sharp, so that a swelling front can be observed. The role of stresses and strains on polymer deformation during diffusion is receiving increasing attention, and recently elastic models have been developed to relate the stress in the polymer to strains generated because of deformations and the presence of the penetrant.[9,10] Petropolous and Roussis[11,12] have been able to predict front formation simply by a concentration-dependent diffusion coefficient with relaxation.

In this paper, we extend the swelling front models by including a phenomenon that has been overlooked in all previous analysis of solute transport in glassy polymers. When the density of the swollen polymer is much less than the density of the glass, a significant convective mass-average velocity can be generated within the sample. This convective velocity in turn will affect the transport of solute in two different ways. First, it will make the convective flux in the species continuity equation of the same order of magnitude as the diffusive flux term and thus nonnegligible. Second, it will make the velocity of the external swollen polymer/solvent front be as fast as that of the swollen polymer/glassy core front velocity. The calculations will show that for reasonable parameter values significant errors can be generated in estimating the sample thickness if these effects are neglected.

In the model used in this paper, we consider the diffusion coefficient to be a function of concentration only, and we use a constitutive equation for the front velocity that depends only on the solute concentration at the glass/swollen polymer interface.[13] Of course, this automatically decouples the effect of the stress fields on the diffusive fluxes. The problem remains mathematically parabolic, and as such, one cannot expect any wavelike behavior in the concentration or the diffusive fluxes. Experimentally one can in fact find situations in which the mass of solute absorbed can oscillate with time. This is apparently due to relaxation effects in the polymer. We also consider the motion of the polymer to be one dimensional so that the continuity equation for total mass and the solute species continuity equation determine both the velocity and solute concentration profiles. These simplifications were made so that the computed velocity fields could be used to calculate the transient strain field in the sample as well as the local state of stress. The stress calculation is based on a linear viscoelastic model with constant parameter values, and it will illustrate very effectively that, in this two-component system, there exists a significant difference between

stresses and strains acting on the polymer only and stresses and strains based on the total or mass-average velocity gradients. This is an issue that has received little attention in the past but that may be a crucial consideration in the development of constitutive equations relating diffusion fluxes to states of stress and strain in the system.

SOLUTE CONCENTRATION AND VELOCITY FIELDS

Mathematical Formulation

Consider a slab of initial thickness 2δ and infinite in the y and z directions immersed in a solute at time $t = 0$, as shown in Fig. 1. As the solute diffuses into the polymer, a swelling front is generated whose position is $x = x_1(t)$ and whose velocity is $-w_1(t)$. In the meantime, the swollen polymer/solution interface is found at $x = x_2(t)$, and it moves at a velocity $w_2(t)$. We need only concern ourselves with the diffusion process along the positive x direction with $x_1(t) < x < x_2(t)$ since the concentration field will be symmetrical about $x = 0$.

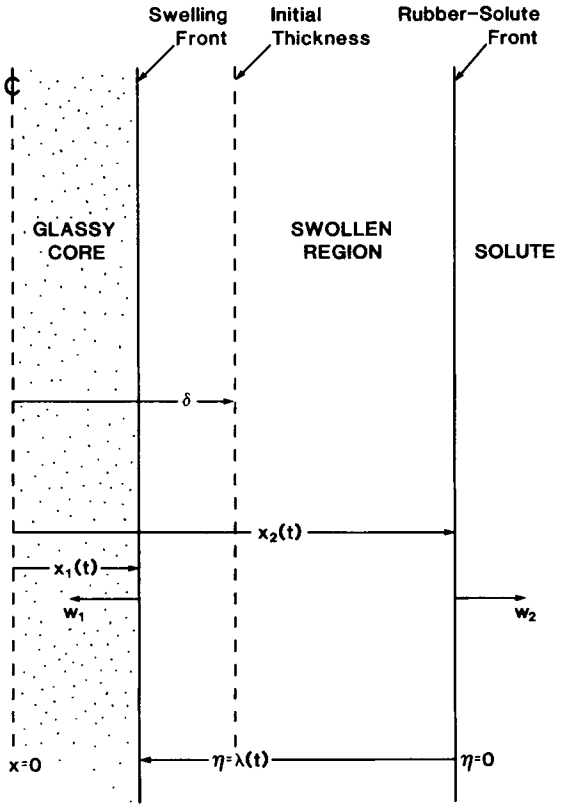

Fig. 1. Coordinate system used for the analysis.

The density of the polymer-solute mixture will depend on the local concentration of solute, so that

$$\rho = \rho(\omega) \qquad \rho = \rho_G \qquad \omega \to 0$$
$$\rho = \rho_S \qquad \omega \to 1 \tag{1}$$

where ρ_S and ρ_G are the pure solute and glass densities. We assume that the local value of the solute concentration will automatically fix the local density so that the variation of the solute concentration with position and time will generate a mass-average velocity according to the continuity equation for total mass:

$$\frac{\partial \rho}{\partial t} = -\frac{\partial}{\partial x}(\rho v) \tag{2}$$

where v is the x component of the mass-average velocity. If the diffusion coefficient is only a function of concentration,

$$\mathscr{D} = \mathscr{D}(\omega) \tag{3}$$

the solute species continuity equation will govern the solute concentration field in the sample

$$\rho(\omega)\frac{D\omega}{Dt} = \frac{\partial}{\partial x}\left(\rho(\omega)\mathscr{D}(\omega)\frac{\partial \omega}{\partial x}\right) \tag{4}$$

Thus, constitutive equations (1) and (3) and the transport equations (2) and (4) are sufficient to calculate $v(x, t)$ and $\omega(x, t)$ once proper boundary conditions are imposed at $x = x_1(t)$ and $x = x_2(t)$.

At $x = x_1(t)$, the concentration of solute in the glass is taken to be zero so that the mass flux of solute in the rubber must be equal to the mass flux of solute convected away from the interface by the front velocity. Thus, the jump mass balance on solvent at $x = x_1(t)$ becomes

$$\rho\omega v_f = \rho\omega v_S = \rho\omega v - \rho\mathscr{D}\frac{\partial \omega}{\partial x} \qquad x = x_1(t) \tag{5}$$

where v_S is the x component of the velocity of the solute and v_f is the x component of the front velocity. Since the glass is taken to be nondeformable, a jump total mass balance at $x = x_1(t)$ results in

$$v = v_f\left(1 - \frac{\rho_G}{\rho}\right) \qquad x = x_1(t) \tag{6}$$

Combining eqs. (5) and (6), we have

$$v_f = -\frac{\rho}{\rho_G}\frac{\mathscr{D}}{\omega}\frac{\partial \omega}{\partial x} \qquad x = x_1(t) \tag{7}$$

The front velocity we take to be a linear function of the concentration of solute[13]:

$$v_f = -w_1 = -k(\omega - \bar{\omega}) \tag{8}$$

so eq. (7) becomes

$$k(\omega - \bar{\omega}) = \frac{\rho}{\rho_G} \frac{\mathcal{D}}{\omega} \frac{\partial \omega}{\partial x} \qquad x = x_1(t) \tag{9}$$

This is the boundary condition for ω at $x = x_1(t)$. The concentration ω at $x = x_1(t)$ is computed from the field equation and the boundary condition in eq. (9). This concentration is time dependent, and as a result, the front velocity v_f is also time dependent through eq. (8). Of course, the location $x_1(t)$ changes according to the kinematic condition

$$\frac{dx_1(t)}{dt} = -w_1 = -k(\omega - \bar{\omega}) \tag{10}$$

At the surface $x = x_2(t)$, we can use the fact that the polymer does not dissolve in the solute to derive an equation analogous to eq. (5) from the jump mass balance on the polymer at $x = x_2(t)$:

$$v_P = w_2 = v + \frac{\mathcal{D}}{1 - \omega} \frac{\partial \omega}{\partial x} \qquad x = x_2(t) \tag{11}$$

Since the location of the swollen polymer/solute interface is given by

$$\frac{dx_2(t)}{dt} = w_2 \tag{12}$$

then eqs. (11) and (12) serve to locate the point $x_2(t)$. At the rubber/solute interface the solute concentration is taken to be the constant

$$\omega = \omega_m \tag{13}$$

For computational purposes, we calculate the density of the rubber and the diffusion coefficient by the equations

$$\frac{1}{\rho} = \frac{(1 - \omega)}{\rho_G} + \frac{\omega}{\rho_S} \tag{14}$$

and

$$\mathcal{D}(\omega) = \mathcal{D}_m \exp\left[\beta(\omega - \omega_m)\right] \tag{15}$$

where $\mathcal{D}_m$ is the diffusion coefficient when $\omega = \omega_m$. Note that the density decreases with increasing solute concentration but the diffusivity increases

if $\beta > 0$. The total thickness of the swollen layer is $\lambda(t)$, and this can be easily calculated:

$$\lambda(t) = x_2(t) - x_1(t) = \int_0^t (w_1 + w_2)\, d\xi \tag{16}$$

We can facilitate the necessary computations if we put the problem in dimensionless form and transform the equations to a frame moving with the rubber/solute interface. In this new frame that surface remains fixed, and the only moving boundary is the glass/rubber swelling front. As a result, consider the transformation

$$\eta = x_2(t) - x \qquad 0 \leq \eta \leq \lambda(t) \tag{17}$$

It is not hard to show that derivatives of any function $\psi(x, t)$ can be related to derivatives in the new coordinate system by the relations

$$\begin{gathered} \psi(x, t) \rightarrow \hat{\psi}(\eta, t) \\ \left(\frac{\partial \psi}{\partial x}\right)_t = -\left(\frac{\partial \hat{\psi}}{\partial \eta}\right)_t \\ \left(\frac{\partial \psi}{\partial t}\right)_x = \left(\frac{\partial \hat{\psi}}{\partial t}\right)_\eta + w_2 \left(\frac{\partial \hat{\psi}}{\partial \eta}\right)_t \end{gathered} \tag{18}$$

The following characteristic quantities may be used to define the dimensionless variables:

$$\begin{aligned} \delta &= \text{characteristic length (original half-width of sample)} \\ v_0 &= k(\omega_m - \bar{\omega}) = \text{characteristic velocity (front velocity when } \omega = \omega_m) \\ t_0 &= \delta / v_0 = \text{characteristic time (time for fronts to meet at center of solid if } \omega = \omega_m) \\ \rho_G &= \text{characteristic density (density of glass)} \end{aligned} \tag{19}$$

The dimensionless variables are defined according to the relations

$$\eta^* = \frac{\eta}{\delta} \qquad 0 \leq \eta^* \leq \frac{\lambda(t)}{\delta}$$

$$v^* = \frac{v}{v_0}$$

$$t^* = \frac{t}{t_0}$$

$$\rho^* = \frac{\rho}{\rho_G} \tag{20}$$

$$w_1^* = \frac{w_1}{v_0}$$

$$w_2^* = \frac{w_2}{v_0}$$

$$\lambda^* = \frac{\lambda(t)}{\delta}$$

Upon transformation to the new coordinate system and using the definitions in eq. (20), the governing equations and boundary conditions for the concentration and dimensionless velocity are given in Table I. Several important dimensionless parameters arise whose values affect the overall system behavior. These are defined by the equations

$$R = \frac{\rho_S}{\rho_G}$$

$$\mathrm{Pe} = \frac{v_0\,\delta}{\mathscr{D}_m} \tag{21}$$

$$\Delta\omega = \omega_m - \bar{\omega}$$

where Pe is the (penetration number). It is clear that to obtain numerical results for the equations in Table I we need to fix the values of Pe, R, $\Delta\omega$, $\bar{\omega}$, and β. In all our computations we have chosen $\beta = 3$ and $\bar{\omega} = 0.05$. This leaves Pe, R, and $\Delta\omega$ as the parameters to be varied. The penetration number Pe is the ratio of the front velocity to the velocity for diffusion. As $\mathrm{Pe} \to \infty$, the concentration profiles should be very steep in the rubber phase; as $\mathrm{Pe} \to 0$, the concentration of solute becomes nearly uniform in the swollen layer. The parameter R is a measure of the overall capacity of the system to generate velocity gradients. As $R \to 1$, the rubber and the glass will have the same density and the mass-average velocity remains constant with position according to the continuity equation. As $R \to 0$, there is a significant density change due to swelling. The parameter $\Delta\omega$ is a measure of the capacity of the polymer for absorbing solute.

Once the v^* and ω fields are known, we can calculate several macroscopic variables associated with the swelling process. Of course, the dimensionless thickness of the swollen layer is $\lambda^*(t^*)$. The total amount of solute absorbed after time t per unit area of sample is

$$M(t) = \int_{x_1(t)}^{x_2(t)} \rho\omega\, dx$$

TABLE I
Dimensionless Form of the Transport Equations and Boundary Conditions for the Velocity and the Concentration Fields

Overall continuity equation:

$$\frac{\partial \rho^*}{\partial t^*} + w_2^* \frac{\partial \rho^*}{\partial \eta^*} = \frac{\partial}{\partial \eta^*}(\rho^* v^*)$$

Solute continuity equation:

$$\rho^* \left[\frac{\partial \omega}{\partial t^*} + (w_2^* - v^*) \frac{\partial \omega}{\partial \eta^*}\right] = \frac{\partial}{\partial \eta^*}\left(\rho^* \mathcal{D}^* \frac{\partial \omega}{\partial \eta^*}\right)$$

Constitutive equations:

$$\frac{1}{\rho^*} = (1 - \omega) + \frac{\omega}{R}$$

$$\mathcal{D}^* = \frac{1}{\mathrm{Pe}} \exp[\beta(\omega - \omega_m)]$$

Boundary conditions:

$$\eta^* = 0 \qquad \omega = \omega_m$$

$$w_2^* = v^* - \frac{\mathcal{D}^*}{1 - \omega} \frac{\partial \omega}{\partial \eta^*}$$

$$\eta^* = \lambda^*(t^*) \qquad \frac{d\lambda^*}{dt^*} = w_1^* + w_2^*$$

$$w_1^* = -\frac{\omega - \bar{\omega}}{\omega_m - \bar{\omega}} = -\frac{\omega - \bar{\omega}}{\Delta\omega}$$

$$v^* = -w_1^*(1 - \rho^{*-1})$$

$$w_1^* = +\frac{\rho^* \mathcal{D}}{\omega} \frac{\partial \omega}{\partial \eta^*}$$

Transforming to the moving frame and making the expression dimensionless, we find

$$M^*(t^*) = \frac{M(t)}{M_G} = \int_0^{\lambda^*(t^*)} \rho^* \omega \, d\eta^* \tag{22}$$

where M_G is the mass of glass per unit area of sample $\rho_G \delta$. The distance penetrated by the swelling front is defined as $\lambda_G = \delta - x_1(t)$, and it is a measure of the velocity of the rubber/glass front. In dimensionless form we can define this penetration depth as

$$\lambda_G^* = \frac{\lambda_G}{\delta} = 1 - \frac{x_1(t)}{\delta} \tag{23}$$

where the right-hand side may be computed from w_1^*.

In addition to these quantities we can also compute the velocity associated with the polymer molecules in the rubber phase. The total or mass average velocity is defined as

$$v = \omega v_S + (1 - \omega) v_P \tag{24}$$

and according to Fick's law of diffusion,

$$v_S = v - \omega \mathcal{D} \frac{\partial \omega}{\partial x} \tag{25}$$

Combining eqs. (24) and (25), we have

$$v_P = \frac{\omega}{1 - \omega} \mathcal{D} \frac{\partial \omega}{\partial x} \tag{26}$$

so that transforming into the moving frame and putting the velocity in dimensionless form we have

$$v_P^* = \frac{v_P}{v_0} = - \frac{\omega}{1 - \omega} \mathcal{D}^* \frac{\partial \omega}{\partial \eta^*} \tag{27}$$

From a knowledge of the concentration field it is then possible to calculate the velocity of the polymer. Note that the polymer will move (swell) even if the convective terms are zero (namely, even if $v^* = 0$). Of course, once the mass-average velocity and the polymer velocity are known, it becomes possible to calculate the associated strains. However, we will reserve the analysis of resulting stresses and strains in the polymer and in the mixture until a later section and turn our attention to the results obtained from the solution of the equations in Table I.

RESULTS FOR ω and v^*

As was mentioned in the previous section, the problem as posed in Table I contains the parameters Pe, R, $\Delta\omega$, $\bar{\omega}$, and β. In all our calculations we have let $\beta = 3$ and $\bar{\omega} = 0.05$, chosen arbitrarily. In this way we can concentrate on the effects of the penetration number (Pe), the density ratio R, and the absorptive capacity $\Delta\omega$ on the rate of transport and swelling. In choosing the magnitude of these parameters, we can rely on typical orders of magnitude for a polymer-solute pair, such as n-hexane-polystyrene, where $0.6 \leq \rho_S \leq 1$ g/cm^3 depending on the pressure, $0.9 \leq \rho_G \leq 1.2$ g/cm^3, $10^{-5} \leq \mathcal{D} \leq 10^{-9}$cm^2/s, $0.15 \leq \omega_m \leq 0.40, \bar{\omega} \simeq 0.05$, and $k \simeq 10^{-6}$ cm/s. A typical initial sample width would be $\delta \simeq 1$ mm. These values help us to provide a reasonable range for the required parameters:

$$10^{-2} \leq \text{Pe} \leq 10^2 \qquad 0.6 \leq R \leq 1 \qquad 0.1 \leq \Delta\omega \leq 0.35$$

Clearly, the penetration number is the quantity subject to the largest possible variation.

The numerical method used was similar to that described by Gostoli and Sarti.[5] The equations were finite differenced in an equally spaced grid, and an iterative procedure was followed in order to compute time increments, concentration profiles, and velocity profiles.

In Fig. 2 we see how the thickness of the rubber or swollen polymer layer changes with time, as well as the time variation of the penetration depth. The values of the parameters are shown in the table in the figure. It is clear that as the ratio of the densities R increases, there is less of a tendency of the material to swell (smaller values of λ^* at a fixed time). Even though when $\rho^* = 1$ (the glass density is equal to the rubber density) the velocity $v^* = 0$, there is still swelling since $v_p^* \neq 0$. This can be seen from eq. (27), since the existence of v_p^* does not depend on the existence of v^*. However, as R increases, the velocity of the glass/swollen polymer front decreases. As a result, the difference between the curves of λ^* and λ_G^* increases as the density difference between glass and polymer increases and as the capacity for solute adsorption increases. The difference $\lambda^* - \lambda_G^*$ can be easily related to the total sample thickness

$$\lambda^* - \lambda_G^* = \frac{x_2(t)}{\delta}$$

When Pe increases, the diffusional resistance is high, and this lowers the concentration of solute near the swelling front. The lower concentration causes the front velocity to decrease and less swelling to occur. This explains the much smaller swelling thickness and overall sample thicknesses for case 4 in Fig. 2 compared with case 3.

Case $R = 1$ is of interest because, as shown in Table I, $v^* = 0$. This is a case for which there are no convective terms in the equation. If one compares curves in which $R = 1$ to curves in which $R < 1$ in Fig. 2, we see that the

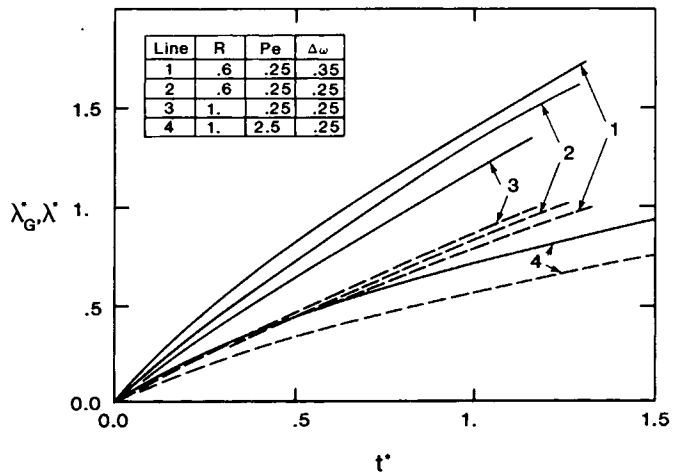

Fig. 2. Swollen layer thickness λ^* (———) and penetration depth λ_G^* (-------) for various parameter valves.

R = 1 case shows much less swelling. Thus, the influence of convective terms is, in general, to increase the rate of swelling of the material. In Fig. 3, the weight uptake M^* is shown for various values of Pe, $\Delta\omega$, and R. Note that they all exhibit case II behavior, in which the mass uptake is a linear function of t^* instead of a linear function of $\sqrt{t^*}$. When the penetration number increases, the mass uptake decreases significantly because of the higher diffusional resistance, regardless of the value of R. Also, the larger the value of $\Delta\omega$, the larger is the weight uptake per unit time, as can be expected. For all the cases shown in Figs. 1 and 2, the concentration profiles have the expected monotonically decreasing shapes from ω_m at $\eta^* = 0$ to a lower value of ω at $\eta^* = \lambda^*(t^*)$. A few examples are shown in Fig. 4.

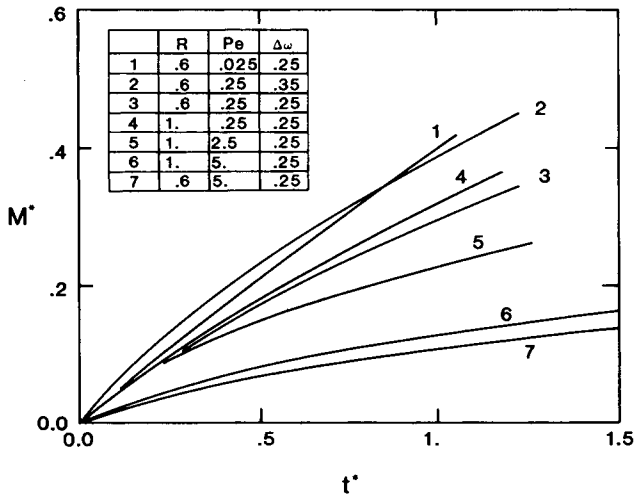

Fig. 3. Weight uptake as a function of time for various parameter values.

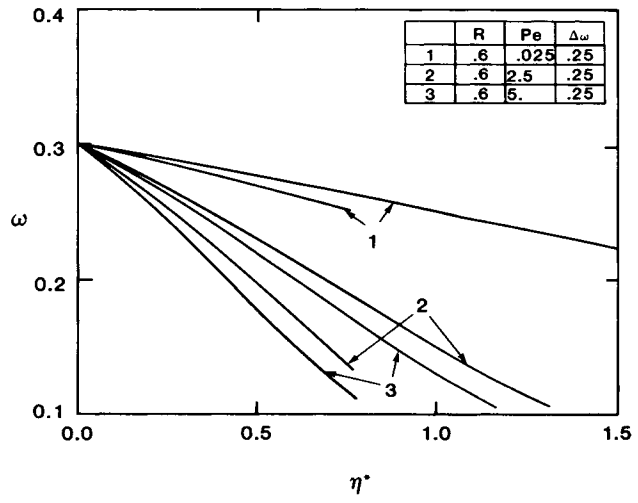

Fig. 4. Typical solute concentration profiles. For each set of parameter values there are two curves corresponding to different t^* values.

In agreement with our previous discussion on the influence of the Pe number, we see that, for small penetration numbers, the drop in the concentration through the rubber phase is relatively small. However, for large values of the penetration number, there is a significant difference between the surface concentration and the concentration at the swelling front. In Fig. 4, for each Pe value there are two curves corresponding to the concentration profiles for two different times. These curves show that the rate of penetration of the swelling front is strongly dependent on the concentration field. The front velocity is governed by the concentration of solute at the glass/rubber interface according to eq. (8).

It is of interest to take a look at the profiles for the mass-average velocity as well as the polymer velocity. In Figs. 5 and 6 we have these quantities plotted as a function of η^* for various parameter values at two different values of time t^*. Note that the polymer velocity is always positive and decreases in the direction of the rubber/glass front. This means that the polymer expands outward from the center of the sample and its velocity is higher as the swollen polymer/solution interface is reached. However, the mass-average velocity seems to go through a maximum, which is more obvious the larger the value of the penetration number (or the larger the diffusional resistance). From eq. (27) we can see that, as ω increases toward the outer edge of the sample, the fraction $\omega/(1 - \omega)$, as well as $\mathcal{D}^*$ becomes larger. Since $\partial\omega/\partial\eta^*$ is negative and nearly constant, then v_p^* increases monotonically as η^* goes to zero. The maximum in v^* is less obvious. However, note that eq. (2), the total continuity equation, may be rewritten as

$$\frac{\partial v}{\partial x} = -\frac{1}{\rho}\frac{\partial \rho}{\partial \omega}\left(\frac{\partial \omega}{\partial t} + v\frac{\partial \omega}{\partial x}\right)$$

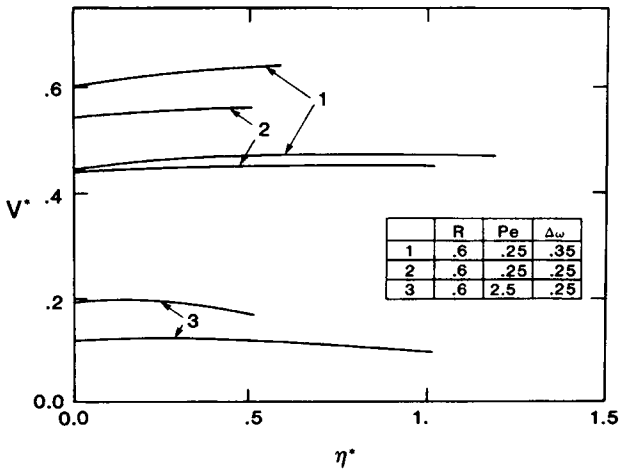

Fig. 5. Mass-average velocity profiles. There are two curves for each set of parameter values, corresponding to two different t^* values.

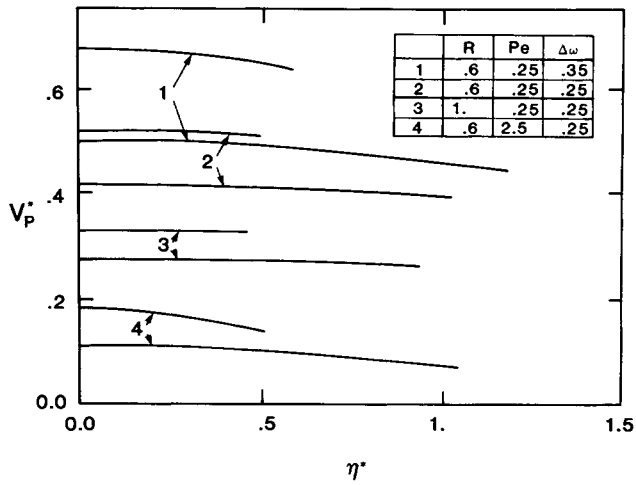

Fig. 6. Polymer velocity profiles. There are two curves for each set of parameter values, corresponding to two different t^* values.

so that transforming to the moving frame and making it dimensionless we obtain

$$\frac{\partial v^*}{\partial \eta^*} = \frac{1}{\rho^*}\frac{\partial \rho^*}{\partial \omega}\left[\frac{\partial \omega}{\partial t^*} + (w_2^* - v^*)\frac{\partial \omega}{\partial \eta^*}\right]$$

At $\eta^* = 0$, $\partial\omega^*/\partial t = 0$, and $w_2^* - v^* = -\mathcal{D}^*/(1 - \omega)\,\partial\omega/\partial\eta^*$ (see Table I). Thus the derivative of v^* at $\eta^* = 0$ is given by

$$\frac{\partial v^*}{\partial \eta^*} = -\frac{1}{\rho^*}\frac{\partial \rho^*}{\partial \omega}\frac{\mathrm{Pe}}{1 - \omega_m}\left(\frac{\partial \omega}{\partial \eta^*}\right)^2 \geq 0 \tag{28}$$

At $\eta^* = \lambda^*$ the term $\partial v^*/\partial\eta^*$ can be either positive or negative, depending on the value of ρ^*, $\mathcal{D}^*$, and the other parameters. In Fig. 4 we see that the result of eq. (28) is verified, even though it is not possible to make a direct prediction of when v^* will go through a maximum as a function of η^*.

In summary, we see that the influence of the convective terms in the equations for solute transport is to have a significant effect on the rate of swelling, especially when the penetration numbers are high and the diffusional resistances dominate. In the next section we look at the types of strains and stresses that would be generated by this motion if we use a linear viscoelastic model for the material deformation.

STRAIN AND STRESSES IN THE MATERIAL

Mathematical Formulation

Now that we have computed velocity fields and concentration profiles during the diffusion of the solute into the polymer, it is of interest to calculate

the strains and stresses that result from this motion. In particular, we are interested in the nonlinear viscoelastic response to the relatively large deformations occurring during the process. Thus, we need to solve equations for the eulerian strain as well as the stress as computed from a corotational Maxwell model for the material. The stress due to material deformations is in general viscoelastic, and for illustrative purposes we can adopt a generalized Maxwell model using upper convected derivatives for the deformation[14]

$$\frac{1}{G}\frac{\delta\boldsymbol{\tau}}{\delta t} + \frac{1}{\mu}\boldsymbol{\tau} = 2\mathbf{D} \tag{29}$$

where G and μ are material constants corresponding to a Young's modulus and a viscosity, respectively. Here, the upper convected derivative is defined as[12]

$$\frac{\delta\boldsymbol{\tau}}{\delta t} = \frac{D\boldsymbol{\tau}}{Dt} - (\nabla\mathbf{v}\cdot\boldsymbol{\tau} + \boldsymbol{\tau}\cdot\nabla\mathbf{v}^T) \tag{30}$$

and the tensor $\mathbf{D}$ is the rate of strain tensor

$$\mathbf{D} = \frac{1}{2}(\nabla\mathbf{v} + \nabla\mathbf{v}^T) \tag{31}$$

As written, the rate of strain is in terms of the mass-average velocity. However, it is not clear whether in fact the stress should be related to the deformation or rate of strain of the *polymer only*. It is possible to define a deformation stress based on the *polymer rate of strain* by an analogous equation,

$$\frac{1}{G}\frac{\delta\boldsymbol{\tau}_p}{\partial t} + \frac{1}{\mu}\boldsymbol{\tau}_p = 2\mathbf{D}_p \tag{32}$$

where

$$\frac{\delta\boldsymbol{\tau}_p}{\delta t} = \frac{D_p\boldsymbol{\tau}_p}{Dt} - (\nabla\mathbf{v}_p\cdot\boldsymbol{\tau}_p + \boldsymbol{\tau}_p\cdot\nabla\mathbf{v}_p^T) \tag{33}$$

with

$$\frac{D_p}{Dt} = \frac{\partial}{\partial t} + \mathbf{v}_p\cdot\nabla \tag{34}$$

$$\mathbf{D}_p = \frac{1}{2}(\nabla\mathbf{v}_p + \nabla\mathbf{v}_p^T) \tag{35}$$

We can write eqs. (29) and (32) for the case of the one-dimensional defor-

mations obtained by the model in Table I. We can transform these equations to the $\eta = x_2(t) - x$ coordinate system, and we can make the equations dimensionless using the characteristic values chosen in eq. (19). The end result of these manipulations is given in Table II.

The stresses have all been made dimensionless using G, so that

$$\boldsymbol{\tau}^* = \frac{\boldsymbol{\tau}}{G} \qquad \boldsymbol{\tau}_p^* = \frac{\boldsymbol{\tau}_p}{G} \tag{36}$$

De is the Deborah number, or the ratio of the relaxation time $t_R = \eta/G$ for the polymer to the characteristic time t_0 for the fronts to meet

$$\mathrm{De} = \frac{t_R}{t_0} = \frac{\mu v_0}{G\delta} \tag{37}$$

One of the characteristics of the deformations of polymers caused by solute transport is that they correspond to very large strains. For example, it is possible for the volume of a polymer to increase by 30% or more. This is equivalent to a strain of 0.6–0.7. As a result, small strain approximations may not be adequate, and it is best to rely on strain fields calculated for arbitrarily large deformations. Malvern[14] reports an equation for the components of the eulerian strain tensor, that is, the strain as a function of spatial position and time, which takes the form

$$\frac{D\mathbf{E}}{Dt} = \mathbf{D} - (\mathbf{E} \cdot \nabla\mathbf{v}^T + \nabla\mathbf{v} \cdot \mathbf{E}) \tag{38}$$

TABLE II
Dimensionless Form of the Equations for Stress in the Polymer and in the Mixture

Stress in the mixture:

$$\frac{\partial \tau_{xx}^*}{\partial t^*} + (w_2^* - v^*)\frac{\partial \tau_{xx}^*}{\partial \eta^*} + 2\tau_{xx}^*\frac{\partial v^*}{\partial \eta^*} + \frac{1}{\mathrm{De}}\tau_{xx}^* = -\frac{\partial v^*}{\partial \eta^*}$$

$$\frac{\partial \tau_{yy}^*}{\partial t^*} + (w_2^* - v^*)\frac{\partial \tau_{yy}^*}{\partial \eta^*} + \frac{1}{\mathrm{De}}\tau_{xx}^* = 0$$

$$\tau_{zz}^* = \tau_{yy}^*$$

Stress in the polymer:

$$\frac{\partial \tau_{xxp}^*}{\partial t^*} + (w_2^* - v_p^*)\frac{\partial \tau_{xxp}^*}{\partial \eta^*} + 2\tau_{xxp}^*\frac{\partial v_p^*}{\partial \eta^*} + \frac{1}{\mathrm{De}}\tau_{xxp}^* = -\frac{\partial v_p^*}{\partial \eta^*}$$

$$\frac{\partial \tau_{yyp}^*}{\partial t^*} + (w_2^* - v_p^*)\frac{\partial \tau_{yyp}^*}{\partial \eta^*} + \frac{1}{\mathrm{De}}\tau_{yyp}^* = 0$$

$$\tau_{xxp}^* = \tau_{yyp}^*$$

This is the strain associated with deformations for the mass-average velocity. For the strain associated with the polymer only, we have

$$\frac{D\mathbf{E}_p}{Dt} = \mathbf{D} - (\mathbf{E}_p \cdot \nabla \mathbf{v}_p{}^T + \nabla \mathbf{v}_p \cdot \mathbf{E}) \tag{39}$$

In the one-dimensional case treated here, the only strain is along the x direction. If we take the equations for the x components of the strains, transform them to the moving frame, and make the equations dimensionless, we have for the mixture strain

$$\frac{\partial E}{\partial t^*} + (w_2^* - v^*)\frac{\partial E}{\partial \eta^*} - 2\frac{\partial v^*}{\partial \eta^*}E = -\frac{\partial v^*}{\partial \eta^*} \tag{40}$$

and for strain on the polymer we have

$$\frac{\partial E_p}{\partial t} + (w_2^* - v_p^*)\frac{\partial E_p}{\partial \eta^*} - 2\frac{\partial v_p^*}{\partial \eta^*}E_p = -\frac{\partial v_p^*}{\partial \eta^*} \tag{41}$$

It is understood that E and E_p refer to the x components of the tensors E and E_p. Since v_p^* and v^* have much different dependencies on η^*, as well as different magnitudes, we can expect E and τ^* to be much different from E_p and τ_p^*.

Before discussing the nature of the results, we have to apply initial and boundary conditions for the stress and strain equations. These can be obtained from some simple considerations of the swelling mechanism applied at the glass/rubber front. The strain acting on the mixture at the rubber/glass interface is given by

$$E_{0,x} = (\rho^*)^{-2/3} - 1 \qquad E_{0,y} = (\rho^*)^{2/3} - 1 \tag{42}$$

and the strain acting on the polymer is

$$E_{0,xp} = (\rho^*)^{-2/3}(1 - \omega)^{-1} - 1 \qquad E_{0,yp} = (\rho^*)^{2/3}(1 - \omega)^{-1} - 1 \tag{43}$$

The corresponding elastic stresses are

$$\tau_{0,xx}^* = 2E_{0,x} \qquad \tau_{0,yy}^* = 2E_{0,y} \tag{44}$$

and

$$\tau_{0,xxp}^* = 2E_{0,xp} \qquad \tau_{0,yyp}^* = 2E_{0,yp} \tag{45}$$

The initial conditions for the stress are that the sample is stressed at the initial interface location by the elastic stresses given in eqs. (44) and (45). The physical picture is that, as soon as the polymer is exposed to the solute, an elastic swelling response is generated, with strains on the mixture and the polymer given by eqs. (42) and (43) and corresponding stresses given by

eqs. (44) and (45). As the swelling front moves, the magnitude of the stresses at the rubber/glass interface changes with time since ρ^* and ω change with time in eqs. (42) and (43).

In Fig. 7 we see the calculated stresses on the mixture for various parameter values. Note that as Pe increases, τ^*_{xx} in general decreases because of the smaller rate of transport of solute into the polymer. When Pe is small (<0.025), the value of the stress at the front is nearly constant in time since the concentration is nearly uniform in the swollen layer. For large Deborah numbers (De), the rubber-phase behavior is nearly elastic. The stress does not relax rapidly away from the front but remains high and can even increase with distance from the front if De is sufficiently high. For high values of both De and Pe, one can see a maximum near the external surface of the rubber. This maximum corresponds to the change in sign of the slope of v^* versus η^* in Fig. 6. This inflection, as we discussed previously, is a direct reflection of the convective terms. One can also see negative values of the stresses τ^*_{xx} close to the external surface. Because of the maximum in the

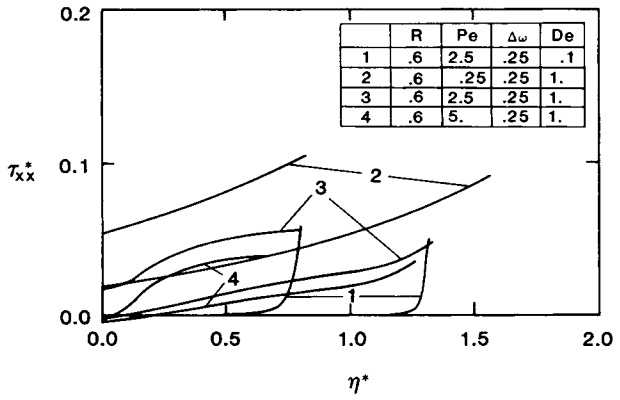

	R	Pe	Δω	De
1	.6	2.5	.25	.1
2	.6	.25	.25	1.
3	.6	2.5	.25	1.
4	.6	5.	.25	1.

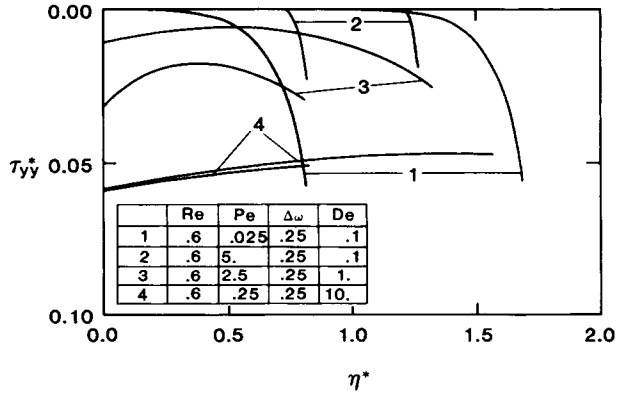

	Re	Pe	Δω	De
1	.6	.025	.25	.1
2	.6	5.	.25	.1
3	.6	2.5	.25	1.
4	.6	.25	.25	10.

Fig. 7. Stress profiles based on mass-average velocity. Two curves corresponding to two different t^* values for each set of parameter values.

mass-average velocity, these stresses can become compressive. The transverse stresses are also shown in Fig. 7. When the Deborah number or Pe is high, τ^*_{yy} does not decrease rapidly away from the glass/rubber interface. It can also have a minimum for the same reason that τ^*_{xx} has a maximum, that is, the change in sign of $\partial v^*/\partial \eta^*$.

In Fig. 8 we show the strain E for a relatively high value of the penetration number. The strain increases away from the rubber/glass front because of the higher concentration of solute (higher swelling) near the solute/rubber interface. When Pe is small, then E is nearly constant with η^* due to the nearly uniform concentration in the rubber phase. The polymer strain E_p is also shown in Fig. 8. Note that E_p is constant at the solute/rubber interface for all time because the material is fully swollen at that point. The value of E_p decreases as the rubber/glass interface is approached.

The stresses felt by the polymer τ^*_{xxp} are shown in Fig. 9 for various values of the important parameters. When the relaxation times are small, the stresses relax to zero quickly, as expected; for large relaxation times the

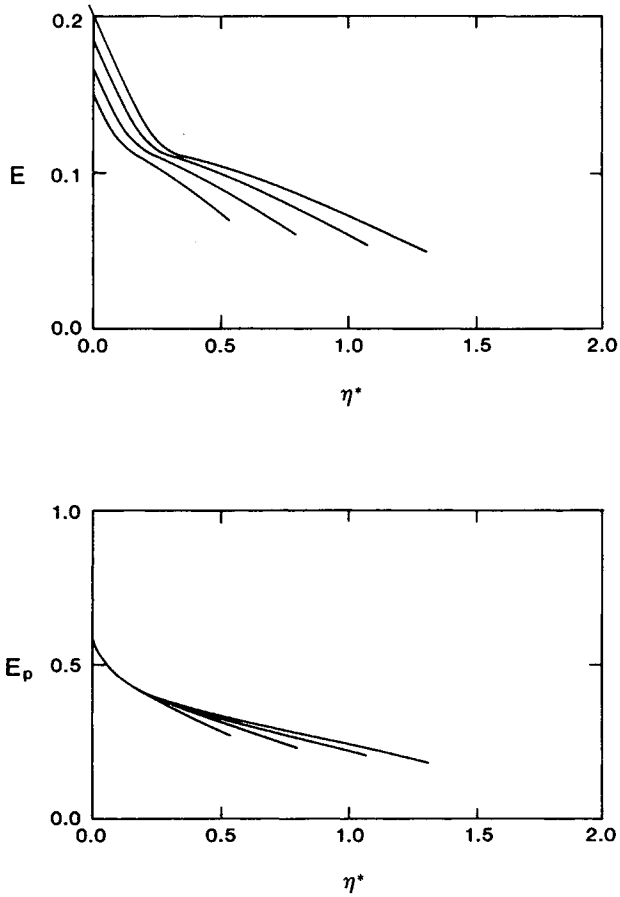

Fig. 8. Strain profile for the mixture and the polymer at different values of t^* (R = 0.6, Pe = 2.5, and $\Delta\omega$ = 0.25).

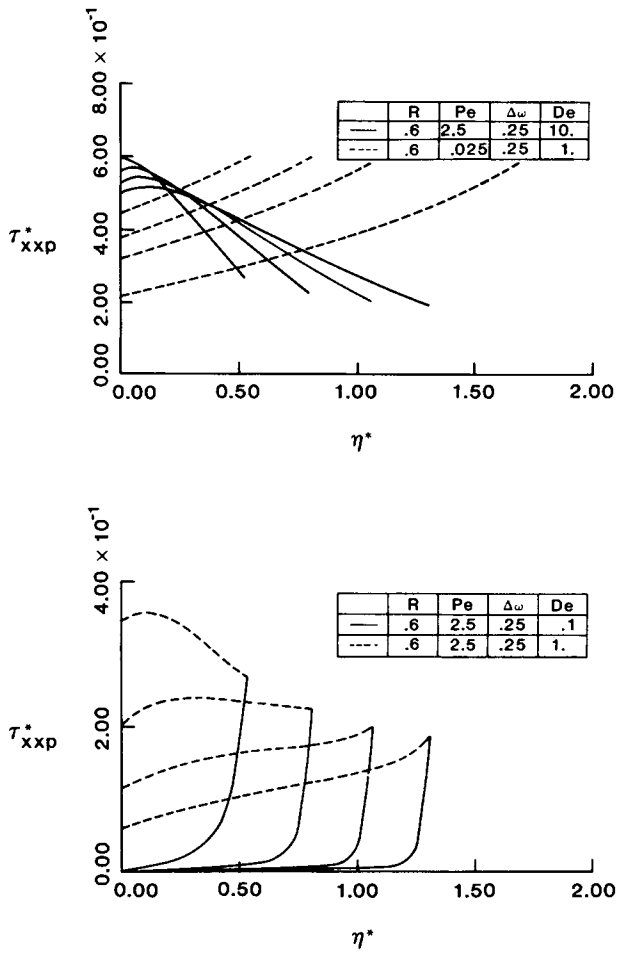

Fig. 9. Stress fields for the polymer for various parameter values and several values of t^*.

stresses do not have time to relax during swelling. When the penetration number is high and there is a large diffusion resistance, the stresses decrease together with the concentration as η^* goes from 0 to its value at the rubber/glass interface. When the penetration number is small, the stresses go through a maximum as one approaches the rubber/solute front because the initially highly stressed rubber has had enough time to relax. The relaxation time is shorter than the diffusion time, and this accounts for the maximum. Note that in the case of τ^*_{xxp} there are no negative values as there are in τ^*_{xx}. A typical strain for the polymer E_p is shown in Fig. 9. Note that the value of E_p near the rubber/solute interface is essentially independent of time since $\partial v^*_p/\partial \eta^* \approx 0$ at that point.

The stresses in the polymer only and in the mixture have quite different manifestations. One can treat the deformation of the material either as a deformation of the mixture of solute and polymer or as the deformation of the polymer only. According to thermodynamic theories of swelling in rubbers, the important aspect of the stresses generated upon deformation is the

stress acting on the polymer chains. This would indicate that in doing dynamic calculations in which the diffusive flux is coupled to the stress, it should be the stress generated in the polymer that governs the swelling process.

CONCLUSIONS

The convective terms in the continuity equation for the solute, in the constitutive equation for stress, and in the kinematic equation for the strain can have a significant influence on the calculated values of the thickness of the swollen layer and the front velocities. They can also influence significantly the computed stresses and strains. The stress and strain fields in the polymer are quite different from the corresponding fields for the mixture. As a result, in treating the kinematics of swelling polymers, great care must be exercised in defining explicitly the reference on which stresses and strains are to be computed.

NOMENCLATURE

$\mathcal{D}$	Molecular diffusivity
$\mathcal{D}^*$	Dimensionless diffusivity
$\mathcal{D}_m$	Maximum diffusivity
De	Deborah number
$\mathbf{E}$	Strain tensor for mixture
$\mathbf{E}_p$	Strain tensor for the polymer
$E_{0,x}$; $E_{0,y}$	Strains in the mixture at the swelling front
G	Elastic modulus
k	Constant in swelling front velocity constitutive equation
M	Mass of solute adsorbed
M_G	Mass of glass per unit area of sample
M^*	Dimensionless mass of solute adsorbed
Pe	Penetration number
R	Ratio of solvent to glass density
t	Time
t_R	Relaxation time for the polymer (μ/G)
t^*	Dimensionless time
t_0	Characteristic time for fronts to meet
v	Velocity in the x direction
v^*	Dimensionless velocity
v_0	Initial velocity of the front
v_p	Velocity of the polymer
v_p^*	Dimensionless velocity of the polymer
v_s	Velocity of the solute
v_f	x component of front velocity ($-w$)
w_1, w_2	Front velocities at rubber/glass and rubber/solute interfaces
w_1^*, w_2^*	Dimensionless front velocities
x	Position along the diffusion direction
x_1, x_2	x components of the glass/rubber and rubber/solute fronts
y	Position normal to the diffusion direction
ω	Weight traction of solute in rubber
$\tilde{\omega}$	Reference weight fraction of solute
ω_m	Maximum weight fraction of solute in rubber
$\boldsymbol{\tau}$	Stress tensor for the mixture
$\boldsymbol{\tau}_p$	Stress tensor for the polymer
η	Coordinate relative to the rubber/solute interface

η^*	Dimensionless coordinate relative to the rubber/solute interface
$\lambda(t)$	Thickness of swollen polymer
β	Constant in constitutive equation for diffusivity
ρ_S	Density of solvent
ρ_G	Density of glass
δ	Initial sample thickness
$\Delta\omega$	Maximum difference in concentration of solute
ρ^*	Dimensionless rubber density
ρ	Rubber density
λ_G	Distance penetrated by the swelling front
λ_G^*	Dimensionless distance penetrated by the swelling front
μ	Viscosity
τ^*, τ_p	Dimensionless stresses in mixture and in polymer

The authors would like to acknowledge the financial support of NATO Research Grant 8410023. The work has also been partially supported by the Italian Ministry of Education. Useful discussions were held with Professors H. B. Hopfenberg and E. Drioli. Their colleagueship was made possible through the NSF U.S.-Italy Binational Cooperative Science Program Grant INT-8219214 held by H. B. Hopfenberg.

References

1. H. B. Hopfenberg, Anomalous transport of penetrants in polymeric membranes, in *Membrane Science and Technology,* J. E. Flinn, Ed., Plenum Press, New York, 1970.
2. H. B. Hopfenberg, R. H. Holley, and V. T. Stannett, *Polym. Eng. Sci.,* **9,** 242 (1969).
3. L. Nicolais, E. Drioli, H. B. Hopfenberg, and D. Tidone, *Polymer,* **18,** 1137 (1977).
4. C. H. M. Jacques, H. B. Hopfenberg, and V. T. Stannett, in *Permeability of Plastic Films and Coatings,* H. B. Hopfenberg, Ed., Plenum Press, New York, 1974.
5. C. Gostoli and G. C. Sarti, *Chem. Eng. Commun.,* **21,** 67 (1983).
6. G. C. Sarti, *Polymer,* **20,** 827 (1979).
7. C. Gostoli and G. C. Sarti, *Polym. Eng. Sci.,* **22,** 1018 (1982).
8. N. L. Thomas and A. H. Windle, *Polymer,* **23,** 529 (1982).
9. M. Kim and P. Neogi, *J. Appl. Polym. Sci.,* **29,** 731 (1984).
10. B. Erman, *J. Polym. Sci.,* **21,** 893 (1983).
11. J. H. Petropolous and P. P. Roussis, *J. Membrane Sci.,* **3,** 343 (1978).
12. J. H. Petropolous and P. P. Roussis, in *Permeability of Plastic Films and Coatings,* H. B. Hopfenberg, Ed., Plenum Press, New York, 1974.
13. G. Astarita and G. C. Sarti, *Polym. Eng. Sci.,* **18,** 338 (1978).
14. L. E. Malvern, *Introduction to the Mechanics of a Continuous Medium,* Prentice-Hall, Englewood Cliffs, New Jersey (1969).